H. pylori Virulence Factor CagA Increases Intestinal Cell Proliferation by Wnt Pathway Activation in a Transgenic Zebrafish Model

James T. Neal[1], Trace S. Peterson[2], Michael L. Kent[2], and Karen Guillemin[3*]

[1] Department of Medicine, Hematology Division, Stanford University School of Medicine, Stanford, CA 94305

[2]Department of Microbiology, Oregon State University, Corvallis, OR 97330

[3]Institute of Molecular Biology, University of Oregon, Eugene, OR 97403

* Corresponding author:

Karen Guillemin

Institute of Molecular Biology

University of Oregon

Eugene, OR 97403

email: guillemin@molbio.uoregon.edu

telephone: 541-346-5360

ABSTRACT

Infection with *Helicobacter pylori* is a major risk factor for the development of gastric cancer, and infection with strains carrying the virulence factor CagA significantly increases this risk. To investigate the mechanisms by which CagA promotes carcinogenesis, we generated transgenic zebrafish expressing CagA ubiquitously or in the anterior intestine. Transgenic zebrafish expressing either wild type or a phosphorylation-resistant form of CagA exhibited significantly increased rates of intestinal epithelial cell proliferation and showed significant upregulation of the Wnt target genes *cyclinD1*, *axin2*, and the zebrafish *c-myc* ortholog *myca*. Co-expression of CagA with a loss-of-function allele encoding the β-catenin destruction complex protein Axin1 resulted in a further increase in intestinal proliferation, while co-expression of CagA with a null allele of the key β-catenin transcriptional cofactor Tcf4 restored intestinal proliferation to wild-type levels. These results provide in vivo evidence of Wnt pathway activation by CagA downstream of or in parallel to the β-catenin destruction complex and upstream of Tcf4. Long-term transgenic expression of wild type CagA, but not the phosphorylation-resistant form, resulted in significant hyperplasia of the adult intestinal epithelium. We further utilized this model to demonstrate that oncogenic cooperation between CagA and a loss-of-function allele of *p53* is sufficient to induce high rates of intestinal small cell carcinoma and adenocarcinoma, establishing the utility of our transgenic zebrafish model in the study of CagA-associated gastrointestinal cancers.

TRANSLATIONAL IMPACT

Clinical issue: The pathogenic bacterium *Helicobacter pylori* is a major global health burden, and is has been implicated in a wide range of gastric disorders from inflammation to cancer. In particular, strains of *H. pylori* capable of translocating the bacterial effector protein CagA into host epithelial cells confer the highest risk for the development of gastric cancer. CagA-induced pathogenesis is multifactorial, and in vitro studies have reported different effects in diverse cell lines. Further, CagA-induced oncogenesis is strongly associated with variations in host genotype, necessitating an in vivo model that faithfully recapitulates human disease mechanisms and is highly genetically tractable.

Results: In this manuscript, we report the development of a novel transgenic zebrafish system for the study of the *H. pylori* virulence factor CagA that recapitulates the major hallmarks of CagA pathogenesis observed in cell culture and murine models, while providing distinct advantages over these models. We report the use of this novel model system to show that activation of canonical Wnt signaling upstream of the β-catenin cofactor Tcf4 and downstream of or in parallel to the β-catenin destruction complex is required for CagA's early effects on intestinal epithelial proliferation. We further report the use of our transgenic zebrafish model to demonstrate CagA's oncogenic potential in combination with a mutant form of the tumor suppressor *p53,* demonstrating that co-expression of CagA and a loss-of-function allele of *p53* results in high rates of neoplastic transformation, and providing the first direct in vivo evidence for oncogenic cooperation between CagA and *p53.*

Implications and future directions: The CagA transgenic zebrafish model described herein presents several key advantages over current in vivo models. First, the rapid development of the zebrafish digestive tract makes it an ideal system for the study of CagA-associated gastrointestinal disease. Second, the ease of transgenesis via Tol2 transposition enables the rapid introduction of additional alleles or structure-function studies that are difficult in other vertebrate models. Finally, the microbiota of CagA transgenic zebrafish is readily manipulated or ablated, enabling future CagA gnotobiotic studies.

INTRODUCTION

Helicobacter pylori is a pathogenic Gram-negative bacterium that colonizes over 50% of the world's human population. Colonization with *H. pylori* is linked to numerous gastric disorders including gastritis, peptic ulcer disease, and gastric adenocarcinoma [1]. Although gastric cancer occurs in fewer than 1% of people colonized by *H. pylori* [2], it is still the second most common cause of cancer mortality worldwide [3], and more than 50% of gastric adenocarcinomas can be attributed to infection with *H. pylori* [4]. Most people infected with *H. pylori*, however, do not develop gastric cancer, and the molecular mechanisms underlying this disparity have yet to be fully elucidated.

Although there are many factors that appear to contribute to *H. pylori*'s carcinogenicity, strains that translocate the CagA protein into host cells are significantly more likely to cause gastric cancer than strains

lacking this ability. CagA is one of 28 gene products encoded by the *cag* pathogenicity island (cag PAI), a 40 kb stretch of DNA shown to be present in most strains isolated from patients with severe gastric pathology [5]. During infection with *H. pylori*, CagA is translocated into host cells via a type IV secretion system (TFSS), where it interacts with a multitude of host cell proteins. These interactions have been shown to affect signal transduction pathways, the cytoskeleton, and cell junctions [6].

After translocation into host cells by the *H. pylori* TFSS, CagA can be phosphorylated by Src family kinases on tyrosine residues within conserved Glu-Pro-Ile-Tyr-Ala (EPIYA) motifs [7,8]. Upon phosphorylation, CagA has been shown to induce morphological changes in cultured epithelial cells through interaction with a variety of host-cell proteins such as SHP-2, Met, Csk, Grb2, and ZO-1 [9,10,11,12,13]. In addition to its phosphorylation-dependent effects, CagA has also been shown to interact in a phosphorylation-independent manner with pathways associated with proliferation and inflammation [14]. Although it is not yet clear which of these myriad interactions are required for the development of gastric cancer in persons colonized by *H. pylori*, the ability of CagA to interact with components of the canonical Wnt signaling pathway provides a potential link between CagA's observed oncogenic effects and a host signaling pathway frequently deregulated in gastrointestinal cancers [15].

In addition to its role in early embryogenesis, the canonical Wnt signaling pathway plays a crucial role in regulating the proliferation and homeostasis of gastrointestinal epithelia. In normal stomach and intestinal epithelia, Wnt signaling has been shown to be important for proliferation, stem cell maintenance, and tissue renewal [16,17,18,19,20]. On the other hand, activation of Wnt signaling has been shown to result in cancers of the stomach and colon [21,22,23]. Wnt pathway activity is tightly controlled via regulation of the primary Wnt effector protein β-catenin. β-catenin complexes with E-cadherin to form adherens junctions between epithelial cells, and in the absence of Wnt ligand, is also bound by Axin/APC/Gsk3β in the so-called 'β-catenin destruction complex' where it is targeted for proteosomal degradation. Upon binding of Wnt by the co-receptors Frizzled and LRP, Axin1 is sequestered at the membrane, preventing assembly of the β-catenin destruction complex. This results in cytoplasmic accumulation of β-catenin, and subsequent translocation of β-catenin into

the nucleus. Upon nuclear translocation, β-catenin binds the essential transcriptional cofactor TCF, and initiates transcription of Wnt target genes, including *axin*, *myc*, and *cyclin* genes.

Non-phosphorylated CagA has been previously shown to disrupt the β-catenin/E-cadherin complex in cultured epithelial cells, causing cytoplasmic and nuclear accumulation of β-catenin, and subsequent activation of the Wnt pathway [24,25,26]. Additionally, CagA has been shown to increase signaling through β-catenin via activation of phosphatidylinositol 3-kinase/Akt [14]. Although the mechanisms of CagA's interactions with the Wnt pathway have yet to be fully elucidated, it is clear both that CagA is capable of activating Wnt signaling through β-catenin, and that inappropriate activation of Wnt signaling is potentially oncogenic.

Understanding the wide variety of host cell interactions required for *H. pylori*-induced pathogenesis has necessitated the use of animal models, and to date numerous primate and rodent models have been developed [27,28,29,30]. Although previously unexploited in the study of *H. pylori* pathogenesis, the teleost fish *Danio rerio* (zebrafish) has emerged as a model organism for the study of various human diseases, including leukemia [31], melanoma [32,33], and intestinal neoplasia [34]. In lieu of a stomach, zebrafish possess an anterior digestive compartment known as the intestinal bulb. The zebrafish intestinal bulb epithelium is columnar and non-ciliated like that of the mammalian stomach, and expresses *sox2* and *barx1* [35], two mammalian stomach markers [36,37,38]. Unlike the mammalian stomach, however, it lacks the chief and parietal cell types. Nonetheless, the zebrafish intestinal bulb has been proposed to share a common ontogeny with the mammalian stomach and its renewal is regulated by similar molecular pathways, including the Notch and Wnt pathways [39,40]. Finally, the rapid development of the zebrafish intestinal tract makes it an ideal model for the study of gastrointestinal development and disease [41].

Here, we describe the development of a novel transgenic model system that simplifies the complexity of *H. pylori* infection to study the effects of a single bacterial protein, CagA, on host cell biology in the zebrafish intestine. We report that proliferation in the zebrafish larval intestinal epithelium is increased by transgenic expression of CagA and that this increase occurs independently of CagA phosphorylation. We demonstrate that expression of CagA induces cytoplasmic and nuclear accumulation of the Wnt effector β-catenin, as well as

activation of known Wnt target genes. The genetic tractability of the zebrafish system allowed us to explore genetic interactions between CagA and a number of host signaling pathways. We show that CagA causes proliferation of the zebrafish intestinal epithelium via activation of the canonical Wnt signaling pathway downstream of or in parallel to the β-catenin destruction complex and upstream of the β-catenin transcriptional cofactor Tcf4. Additionally, we demonstrate that long-term expression of wild-type CagA, but not the phosphorylation-resistant form, is sufficient to induce pathologic intestinal hyperplasia in adults, and that oncogenic cooperation between the *cagA* transgene and a loss-of-function allele of *p53* results in high rates of intestinal adenocarcinoma and small cell carcinoma .

RESULTS

Generation of CagA-expressing Transgenic Zebrafish. In order to generate *cagA* transgenic animals, we cloned the *cagA* gene from *H. pylori* strain G27. Strain G27 was originally isolated from Grossetto Hospital (Tuscany, Italy), and has been used extensively in research on the CagA virulence factor [9,24,42,43]. The cloned gene was then 3'-tagged with EGFP to facilitate in vivo visualization of CagA expression. To express CagA ubiquitously in zebrafish, the *cagA/EGFP* fusion construct was connected downstream of the 5.3kb *beta-actin* (*b-*) [44] promoter (Fig. S1A). To facilitate intestine-specific expression of the fusion construct, we connected *cagA/EGFP* downstream of a 1.6kb fragment of the zebrafish *intestinal fatty acid binding protein* (*i-*)[45] promoter (Fig. S1B). By 6 days post-fertilization (dpf) *b-cagA/EGFP* transgenic zebrafish exhibited ubiquitous fluorescence, whereas *i-cagA/EGFP* transgenic larvae exhibited fluorescence in the distal esophagus and anterior intestine (Fig. 1 A and B). CagA's phosphorylation state has been previously shown to have significant effects on the type and severity of CagA-induced pathologies, so in order to determine the role of CagA phosphorylation in the intestinal epithelium, we fused the previously described phosphorylation-resistant $cagA^{EPISA}$ allele [8] (Fig. S1C) to EGFP and connected it downstream of the *b-actin* promoter (Fig. S1D). *b-*$cagA^{EPISA}$*/EGFP* transgenics exhibited ubiquitous fluorescence and were indistinct from *b-cagA/EGFP* fish (Fig. 1C). Expression of *cagA* mRNAs was verified in transgenic animals by RT-PCR (Figure 1D), and analysis

of relative intestinal *cagA* transcript level in the transgenic lines via quantitative real-time PCR revealed significantly elevated expression of the *cagA* transgene when driven by the *b-actin* promoter vs the *i-fabp* promoter (Fig. 1E).

CagA Expression Causes Overproliferation of the Intestinal Epithelium. To determine the effects of CagA expression on the larval zebrafish intestine, we examined wild-type and CagA transgenic animals at 6 dpf, by which time autonomous feeding has begun, and at 15 dpf, by which time intestinal folding is complete [46]. CagA-expressing zebrafish larvae showed normal intestinal development (Fig. 2A and B), and were histologically indiscernible from wild-type clutch-mates (Fig. 2C and D). In addition, the CagA-expressing larvae exhibited no gross abnormalities in cell junctions, as assessed by staining with a pan-cadherin antibody (Figure S2). We next sought to establish CagA's effects on larval intestinal proliferation, as CagA had been previously shown to increase epithelial cell proliferation in vitro and in vivo [13,47]. To determine the proliferation state of CagA-expressing intestines, we analyzed animals at 6 and 15 dpf that had been exposed to the nucleotide analog 5-ethynyl-2'-deoxyuridine (EdU) for approximately 10 hours and counted S-phase nuclei in 30 serial sections of the intestinal bulb. Expression of CagA resulted in a significant increase in EdU labeled cells in all transgenic lines at 6 and 15 days post-fertilization (Fig. 2E & F). To determine if this increase in proliferation had an effect on the cell census, we quantified total epithelial cell number in single H&E-stained sagittal sections along the length of the intestine. We did not observe any significant difference in total cell counts between CagA transgenics and wild-type animals at 6 and 15 dpf (Fig. 2G & H), indicating that expression of CagA caused increased turnover of intestinal epithelial cells. Increased intestinal cell turnover would require an increase in cell death, however, consistent with previous reports and due to the transient nature of extruded apoptotic cells [39], we observed very few TUNEL-positive cells in the intestines of wild-type and CagA-expressing animals (Fig. 2I & J), with no significant difference observed between the two groups. Finally, the intestinal epithelia of *b-cagA* animals did not display an increased number of local neutrophils at 8 dpf, indicating a lack of CagA-induced intestinal inflammation at this stage (Fig. S3).

CagA Expression Activates the Wnt Pathway Downstream of the β-catenin Destruction Complex. We had previously shown that epithelial cell proliferation in the zebrafish intestine is regulated by the Wnt pathway [40]. In addition, previous studies had shown that CagA can induce cytoplasmic and nuclear accumulation of the Wnt effector protein β-catenin, and can activate transcription of canonical Wnt target genes [14,15,47]. Accordingly, we examined whether CagA expression was capable of activating the Wnt signaling pathway in the zebrafish intestine at different developmental stages. We first utilized quantitative real-time PCR to assess the relative expression levels of known Wnt target genes in dissected adult intestines. Transcript levels of the Wnt target genes *c-myc* (*myca*) [48], *axin2* [49], and *cyclinD1* [50] were modestly increased in all CagA-expressing lines relative to the wild-type strain (Fig. 3A-C). We next asked whether CagA was capable of inducing β-catenin accumulation in epithelial cells of the larval intestine, indicating activation of the Wnt pathway. CagA expression caused a significant increase in the number of intestinal epithelial cells with cytoplasmic and nuclear accumulation of β-catenin as compared to wild-type animals (Fig. 3D & E). The fact that EdU labeling was not usually coincident with cytoplasmic and nuclear accumulation of β-catenin is likely due to the fact that whereas relocalization of β-catenin is a transient event, the EdU labeled cells that had undergone S-phase any time during the 12 hour labeling period.

In order to assess the significance of CagA-induced β-catenin accumulation, we next compared the intestinal β-catenin accumulation observed in CagA-expressing animals to that of a known Wnt signaling mutant, *axin1*^{tm213}. *axin1*^{tm213} homozygotes exhibit deregulated Wnt signaling as a result of a missense mutation in the Gsk3β binding domain of Axin1, which prevents assembly of the β-catenin destruction complex. These mutants die as a result of craniofacial defects, but are viable through 8 dpf, allowing study of the juvenile intestine [51,52]. As expected, we observed increases over wild-type and CagA-expressing animals in both the number of proliferating cells and the number of cells featuring cytoplasmic and/or nuclear accumulation of β-catenin in the intestinal epithelia of *axin1*$^{tm213/tm213}$ mutants, consistent with constitutively activated Wnt signaling (Fig. 3E).

We reasoned that if CagA were capable of activating Wnt signaling upstream of the β-catenin destruction complex, then *axin1*^{tm213} homozygotes should be refractory to CagA-induced accumulation of β-catenin, and levels of β-catenin accumulation in *b-cagA*; *axin1*$^{tm213/tm213}$ double mutants should resemble those of *axin1*^{tm213} homozygotes. Instead, when we generated *b-cagA*, *axin1*$^{tm213/tm213}$ fish, we found that expression of CagA in *axin1* homozygous mutants resulted in a dramatic increase in cell proliferation and β-catenin accumulation (Fig. 3F). Taken together, these data indicate that CagA is capable of causing sustained activation of canonical Wnt signaling in the intestinal epithelium, and that it does so either downstream of, or in parallel to the β-catenin destruction complex. Furthermore, CagA-induced accumulation of β-catenin was strongly correlated with increased epithelial proliferation (Fig. 3G & H), suggesting that CagA may stimulate proliferation through activation of the Wnt pathway.

CagA-dependent Overproliferation of the Intestinal Epithelium Requires *tcf4*. To determine if CagA-induced overproliferation of the intestinal epithelium was dependent on canonical Wnt signaling downstream of the β-catenin destruction complex, we utilized a null allele of the essential β-catenin transcriptional cofactor, Tcf4 [35]. We reasoned that if CagA's pro-proliferative effects were acting upstream of Tcf4, rates of intestinal proliferation in *i-cagA; tcf4*^{exl} double mutants should be identical to those observed in *tcf*^{null} animals. As previously observed, *i-cagA* animals showed a significant increase in proliferation over wild-type, whereas *tcf4*$^{exl/exl}$ mutants showed levels of intestinal proliferation similar to wild-type animals (Fig. 4). Rates of intestinal proliferation in *i-cagA; tcf4*$^{exl/exl}$ larvae were statistically indistinguishable from wild-type and *tcf4* $^{exl/exl}$ mutants, indicating that CagA requires Tcf4 function to increase intestinal epithelial proliferation. This result places CagA's activation of the Wnt signaling pathway downstream of or in parallel to Axin1 and upstream of Tcf4 (Fig. S4).

CagA expression causes phosphorylation-dependent intestinal hyperplasia in adult zebrafish. *H. pylori*-associated gastric adenocarcinoma occurs as a result of lifelong exposure to the bacterium, with CagA+ strains

posing a significantly greater cancer risk [4]. In order to study the long-term effects of CagA exposure in our model, we performed histological analysis of adult *b-cagA*, *i-caga*, and *b-caga*^{EPISA} animals at one year of age. Wild-type adults (18 months post-fertilization) served as controls. Upon examination, no hyperplastic or neoplastic lesions were found in any of the wild-type controls (Fig. 5A and G, Table S1). A proportion of the *b-cagA* and *i-cagA* individuals exhibited significant intestinal epithelial hyperplasia at one year of age (Fig. 5 B and C). Surprisingly, despite the significant increases in proliferation and Wnt activation observed in younger *b-caga*^{EPISA} animals, no hyperplasia was observed in age-matched adults of this genotype (Fig. 5D). These data suggest that while the phosphorylation-independent activation of Wnt signaling by CagA is sufficient to induce sustained overproliferation of the larval intestinal epithelium, it is not sufficient to induce significant hyperplastic changes in the adult intestinal epithelium, as seen in the groups expressing the non-mutant CagA, either ubiquitously or in an intestine-specific manner.

Co-expression of the *cagA* transgene with a *p53* loss-of-function allele results in high rates of intestinal adenocarcinoma. The tumor suppressor gene *p53* is frequently mutated in diffuse- and intestinal-type gastric cancers [53,54]**,** and gastric adenocarcinomas isolated from CagA+ *H. pylori*-infected patients exhibit frequent mutation in *p53* [55]. Additionally, CagA has been shown to subvert the tumor suppressor function of the apoptosis-stimulating protein ASPP2 in cultured cells, leading to enhanced degradation of p53 [56]. In order to examine the potential for oncogenic cooperation between the *cagA* transgene and *p53* we bred *b-cagA* and *i-cagA* animals to animals homozygous for a loss-of-function allele of *p53* (*tp53*^{M214K}) to obtain *b-cagA; tp53*$^{M214K/M214K}$ or *i-cagA; tp53*$^{M214K/M214K}$ animals. The zebrafish ortholog of *p53* is highly conserved in both structure and function, and the *tp53*^{M214K} DNA-binding domain mutation is orthologous to methionine-246 missense mutations previously identified in human tumors [57]. At 1 year post-fertilization, all of the *tp53*$^{M214K/M214K}$ fish failed to thrive and exhibited high rates of ocular malignant peripheral nerve sheath tumors, recapitulating previous studies using this *p53* allele [58]. An insufficient number of *b-cagA; tp53*$^{M214K/M214K}$ individuals survived to this time point for analysis, but we were able to examine small numbers of both

tp53$^{M214K/M214K}$ and *i-cagA; tp53*$^{M214K/M214K}$ (Fig. 5 E and F) lines. In both lines, we observed examples of intestinal epithelial hyperplasia and definitive neoplasia (Fig. 5G). In the affected genotypes displaying hyperplastic changes, the intestinal mucosa was thrown into irregular and haphazard folds lined by a ragged and thickened epithelium often 2 to 6 cells deep with pseudostratification of nuclei, which was most prominent within invaginations between the mucosal villi (mucosal sulci). Infolding of the hyperplastic epithelium frequently resulted in formation of mucosal pseudocrypts, with the most severely affected intestines also displaying frequent epithelial fusion between adjacent mucosal folds. In addition, numerous aponecrotic intestinal epithelial cells were observed and directly reflected rapid epithelial cell proliferation and turnover. Small numbers of a chronic inflammatory cell infiltrate, composed mostly of lymphocytes and few eosinophilic granule cells, were seen percolating through the hyperplastic epithelium in many areas. Foci of dysplastic intestinal epithelial cells were often identified in hyperplastic areas, usually within mucosal sulci. Dysplastic cells demonstrated progressive disorganization including "piling-up" of cells and loss of nuclear polarity, nuclear and cytologic pleomorphism, hyperchromatic elongated nuclei and inconspicuous nucleoli with sparse cytoplasm (increased nuclear to cytoplasm ratio) and occasional bizarre mitotic figures. In all cases where dysplastic cells were observed there was no invasion through the basement membrane (i.e., carcinoma in situ) except for one fish in the *tp53*$^{M214K/M214K}$ group, which had a solitary maxillary (upper jaw) focus of carcinoma in situ within the oropharyngeal cavity. When definitive intestinal neoplasia was seen, adenocarcinoma was most often found in the anterior intestine and small cell carcinoma in the anterior or mid-intestine. Adenocarcinomas displayed variable degrees of differentiation, ranging from well to poorly differentiated, with a tendency to form disorganized and cribrose acinar-like pseudocrypts that penetrated deep into the lamina propria, in the absence of an interceding basement membrane. Individual tumor cells had hyperchromatic, ovoid to elongated nuclei with granular chromatin, multiple small nucleoli and sparse basophilic cytoplasm. In less differentiated adenocarcinomas, bizarre mitotic figures were occasionally seen. Locally extensive fibrogenesis within the lamina propria (intraproprial desmoplasia), and variable numbers of chronic inflammatory cell infiltrates, comprised of intermingled lymphocytes and eosinophilic granule cells, were often associated with

the adenocarcinomas. The two small cell carcinomas identified in the *i-cagA; tp53*$^{M214K/M214K}$ group were composed of densely cellular nests of polygonal to fusiform cells, lacking an organoid pattern, which infiltrated deep into the lamina propria and were not associated with pseudocrypts. Individual neoplastic cells within nests had pleomorphic, deeply basophilic nuclei with dense granular chromatin, inconspicuous nucleoli and minimal cytoplasm. Solitary necrotic tumor cells were seen in some of the nests, accompanied by small aggregates of lymphocytes. Lymphovascular invasion and distant metastasis was not observed in either of the tumor types. Incidence and overall severity of lesions within the expression domain of the *cagA* transgene were higher in *i-cagA; tp53*$^{M214K/M214K}$ animals than in the corresponding anatomical region of *tp53*$^{M214K/M214K}$ animals (Fig. 5G and Table S1). These data indicate that expression of CagA with concomitant *p53* loss is sufficient to induce high rates of adenocarcinoma and small cell carcinoma in the zebrafish intestine, and demonstrate the utility of our model for the study of CagA-associated gastrointestinal cancers.

DISCUSSION

Here, we describe the development of a novel in vivo model of CagA-induced intestinal pathology in zebrafish that recapitulates major hallmarks of CagA pathogenesis observed in cell culture and murine models such as increased epithelial proliferation, cellular accumulation of β-catenin, and intestinal hyperplasia [13,24,25,26,29,47]. We utilize transgenic expression of CagA to investigate how the *H. pylori* virulence factor CagA is able to disrupt normal programs of intestinal epithelial renewal via activation of an important host signaling pathway, the Wnt pathway, to cause significant overproliferation of an intact epithelium in vivo. We show that activation of canonical Wnt signaling upstream of the essential β-catenin cofactor Tcf4 and downstream of the β-catenin destruction complex is required for CagA's early effects on intestinal epithelial proliferation.

We further utilized our novel transgenic zebrafish system to demonstrate that long-term expression of CagA is sufficient to cause intestinal hyperplasia in adult zebrafish. Notably, although expression of the phosphorylation-resistant *b-cagA*^{EPISA} allele is capable of inducing significant sustained overproliferation of the

larval intestinal epithelium coupled with increased Wnt activation, it failed to induce significant intestinal hyperplasia in adult animals. These data corroborate a previous study using a CagA transgenic mouse model, which demonstrated the ability of CagA to induce severe epithelial hyperplasia in vivo is correlated with its capacity to be phosphorylated by host kinases [29]. It is possible that CagA's activation of Wnt signaling and subsequent induction of proliferation act in concert with further oncogenic stimuli, which may occur in the form of previously observed phosphorylation-dependent events such as epithelial depolarization [9] or ERK activation by CagA [59]. These data illustrate the utility of long-term in vivo modeling of CagA pathogenesis, as the cumulative effects of CagA expression cannot be predicted from the transient cellular responses it elicits.

Host genetics play a significant role in the development of *H. pylori* associated gastric cancer. For example, certain alleles of the host genes *p53*, *IL-1β*, and *IL-10* are strongly correlated with the development of gastric adenocarcinoma in *H. pylori*-infected humans [55,60]. Transgenic expression of CagA in mice was sufficient to cause gastric and intestinal carcinomas, but these only developed in less than 5% of the animals [29]. We observed high rates of intestinal neoplasia in our CagA transgenic zebrafish model when expressed with a mutant allele of the tumor suppressor *p53*. These data provide the first direct in vivo evidence for oncogenic cooperation between CagA and *p53* and provide a robust model of CagA-induced carcinoma. Our results are consistent with previous findings of increased *p53* mutational frequency in *H. pylori*-associated gastric cancer cases [55] and corroborate a previous study establishing CagA as a bona-fide oncoprotein [29]. More importantly, these data support the use of our model in the screening of putative gastric cancer susceptibility loci for oncogenic cooperation with CagA.

Materials and Methods

Ethics. All zebrafish experiments were carried out in strict accordance with the recommendations in the Guide for the Care and Use of Laboratory Animals of the National Institutes of Health. The University of Oregon Animal Care Service is fully accredited by the Association for Assessment and Accreditation of Laboratory Animal Care and complies with all United States Department of Agriculture, Public Health Service, Oregon State and local area

animal welfare regulations. All activities were approved by the University of Oregon Institutional Animal Care and Use Committee (Animal Welfare Assurance number A-3009-01).

Animals. Transgenic zebrafish were developed using the Tol2kit as previously described [61]. *tp53*^{M214K} [58], and *axin1*^{tm213} [51] animals were obtained from Monte Westerfield (University of Oregon) and *tcf4*^{exI} [35] from Tatjana Piotrowski (University of Utah). All zebrafish experiments were performed using protocols approved by the University of Oregon Institutional Care and Use Committee, and following standard protocols [62]. CagA transgenics may be obtained by contacting the corresponding author.

EdU Labeling and Detection. Zebrafish larvae were immersed in 100 µg/mL EdU (A10044; Invitrogen) with .5% DMSO for 8-12 hours, fixed overnight at 4° C (4% paraformaldehyde in PBS) with gentle shaking, processed for paraffin embedding, and cut into 7µM sections. Slides were then processed using the Click-iT EdU Imaging Kit (C10337, Invitrogen). EdU labeled nuclei within the intestinal epithelium were counted over 30 serial sections beginning at the intestinal-esophageal junction and proceeding caudally into the intestinal bulb.

TUNEL staining. Staining was carried out using the Click-iT TUNEL Imaging Assay (C10245, Invitrogen). TUNEL-positive cells within the intestinal epithelium were counted over 30 serial sections beginning at the intestinal-esophageal junction and proceeding caudally into the intestinal bulb.

Immunohistochemistry. Immunohistochemistry was carried out of paraffin sections as previously described using anti-β-catenin (1:1000, C2206 rabbit polyclonal, Sigma) [40].

Histopathology. Histopathological analysis of H&E stained sections was performed by pathologists with expertise in laboratory fish (TSP and MLK) in a blinded manner. For each adult zebrafish genotype, four consecutive sagittal serial sections of the entire intestinal tract, anterior to posterior, were evaluated for epithelial hyperplasia, dysplasia and the presence of neoplasia. Classification of intestinal epithelial hyperplasia included two or more of the following criteria: epithelial cell nuclear pseudostratification, multi-layering of mucosal fold epithelial cells and formation of pseudocrypts, which indicated extensive infolding of hyperplastic epithelium lining the intestinal mucosal folds. Dysplastic changes of the intestinal epithelial cells, observed in

several fish within the hyperplastic intestinal epithelium, were classified as an increased nuclear to cytoplasm ratio, nuclear hyperchromatism with indiscernible nucleoli, "piling-up" of epithelial cells, loss of nuclear polarity (i.e. loss of basally oriented epithelial cell nuclei) and abnormal mitotic figures. Classification of intestinal adenocarcinoma included the following criteria: Invasive cribriform pseudocrypts that interfaced directly with the lamina propria in the absence of an interceding basement membrane, disorganized histoarchitectural patterns of the pseudocrypts, loss of differentiation from well-defined pseudocrypts to complete absence of acinar-like structures and a desmoplastic response to the neoplastic cells. Small cell carcinoma was classified as densely cellular and discrete small sheets and nests of tumor cells within the lamina propria, with minimal cytoplasm, that lacked an organoid growth pattern. Intratumoral inflammatory infiltrates were also accounted for and classified by chronicity and cell type. Other proliferative lesions, which occurred in only one fish, are described in the results.

Quantitative RT-PCR. Reference gene testing was performed using the geNorm reference gene selection kit (Primerdesign) and qBase^{PLUS} software (Biogazelle). Baseline, threshold, and efficiency calculations were performed using LinRegPCR software [63] Quantitative RT-PCR reactions were performed using the SYBR FAST qPCR kit (Kapa Biosystems) on a StepOnePlus Real-Time PCR System (Applied Biosystems) using primers listed in Table S2. Expression data were normalized to the geometric mean of the reference genes using StepOne (ABI) software.

Myeloperoxidase (mpo) staining. Mpo staining was carried out using the Leukocyte Peroxidase (Myeloperoxidase) Staining Kit (Sigma-Aldrich). Mpo-positive cells within the intestinal epithelium were counted over 30 serial sections beginning at the intestinal-esophageal junction and proceeding caudally into the intestinal bulb.

Statistical Analysis. All statistical analyses were performed with Graph-Pad Prism software.

Acknowledgments

We thank Erika Mittge for technical assistance, Rose Gaudreau and the staff of the University of Oregon Zebrafish Facility for excellent fish husbandry, Poh Kheng Loi and the staffs of the University of Oregon and Oregon State University histology facilities for histology services.

Competing Interests

The authors do not report any competing interests.

Funding

This research was supported by NIH grant 1R01DK075667 (to K.G.) and a Burroughs Wellcome Fund Investigator in the Pathogenesis of Infectious Disease Award (to K.G.). NIH grant HD22486 provided support for the Oregon Zebrafish Facility.

Author Contributions

JTN and KG designed experiments. JTN performed experiments. JTN, TSP, MLK, and KG analyzed data. JTN, TSP, MLK, and KG wrote the paper.

Figure Legends

Fig. 1. Development of CagA+ transgenic zebrafish (A) ubiquitous CagA/EGFP fusion protein expression driven by the *b-actin* promoter. (B) ubiquitous CagA^{EPISA}/EGFP fusion protein expression driven by the *b-actin* promoter. (C) intestinal CagA/EGFP fusion protein expression driven by the *i-fabp* promoter. (Scale bars: A-C, 500 μM) (D) RT-PCR of dissected larval intestine showing expression of *cagA* and *RPL13* housekeeping control gene at 6 dpf. (E) quantitative RT-PCR of dissected adult intestines showing relative expression levels of *cagA* transcript in transgenic lines at 1 year of age. (expression levels normalized to SDHA and β-actin, error bars indicate mean ± SD of biological triplicates)

Fig. 2. CagA expression causes overproliferation of the intestinal epithelium (A and B) H&E stained sagittal sections of wild-type (A) and *b-cagA* transgenic (B) zebrafish intestine at 6 dpf. (C and D) H&E stained sagittal sections of wild-type (C) and *b-cagA* transgenic (D) zebrafish intestine at 15 dpf. (Scale bars: A-D, 10 μM) (E and F) Intestinal epithelial cell proliferation at 6 dpf (E) and 15 dpf (F). Bars represent proliferation as a percentage of wild-type. (n=10, * = p<.05, One-way ANOVA with Tukey's test. Error bars represent SEM.) (G and H) Total intestinal epithelial cell counts of single H&E stained midline sagittal sections at 6 dpf (G) and 15 dpf (H). (I and J) TUNEL-positive cells in the intestinal epithelium at 6 dpf (I) and 15 dpf (J).

Fig. 3. CagA activates canonical Wnt signaling in the intestinal epithelium (A) Quantitative RT-PCR data showing relative expression levels of the Wnt target gene *mycA*. (B) Quantitative RT-PCR data showing relative expression levels of the Wnt target gene *cyclinD1*. (C) Quantitative RT-PCR data showing relative expression levels of the Wnt target gene *axin2*. (expression levels assayed in dissected adult intestines and normalized to SDHA and β-actin, error bars indicate mean ± SD of biological triplicates) (D-G) Immunofluorescence micrograph showing proliferating cells (EdU, green, 10 hour label) and cells with nuclear/cytoplasmic accumulation of β-catenin (red staining & white arrowheads) in intestinal cross-sections of wild-type (D), *b-cagA* (E), *axin1*^{tm213} (F), and *b-cagA; axin1*^{tm213} (G) animals at 6 dpf. (H) Quantification of proliferating (EdU+) cells. (I) Quantification of cells with nuclear/cytoplasmic accumulation of β-catenin.

Fig. 4. CagA-dependent overproliferation of the intestinal epithelium requires *tcf4*. Intestinal epithelial cell proliferation at 15 dpf. Bars represent proliferation as a percentage of wild-type. (n=10, * = p<.05, One-way ANOVA with Tukey's test. Error bars represent SEM.)

Fig. 5. CagA expression causes phosphorylation-dependent intestinal epithelial hyperplasia and induces adenocarcinoma formation in combination with *p53* loss. (A-F) H&E stained sagittal sections of adult zebrafish intestine (Scale bars: A-F, 25μM). (A) Wild-type intestine at 18 months post-fertilization (mpf) showing normal intestinal architecture, with a single layer of epithelial cells lining the mucosal folds. (B & D) *b-cagA* (B) and *i-cagA* (D) intestines at 12 mpf, displaying mucosal fold epithelial hyperplasia, dysplasia within mucosal sulci, and mucosal fold fusion. (C) *b-cagA*^{EPISA} intestine at 12 mpf showing normal intestinal architecture, identical to wild-type. (E) *i-cagA; tp53*$^{M214K/M214K}$ small cell carcinoma with small nests of neoplastic cells in lamina propria (arrow). Inset depicts higher magnification of tumor cells; "x" mark the epithelium in E and F. (F) *i-cagA; tp53*$^{M214K/M214K}$ adenocarcinoma, poorly differentiated, invading into the lamina propria with complete disorganization of the epithelium which is shown by goblet cells randomly scattered throughout (arrows). (G) Summary of intestinal histological abnormalities observed in adult CagA-expressing animals as a result of a blinded histological analysis of H&E stained sections. (wild-type, n=22; b-cagA, n=24; b-cagA^{EPISA}, n=18; i-cagA, n=19; tp53$^{M214K/M214K}$, n=5; i-cagA/tp53$^{M214K/M214K}$, n=7)

Fig. S1. Transgenic constructs (A) The *cagA:egfp* fusion cassette was cloned downstream of the 5.3kb *b-actin* promoter fragment. (B) The *cagA:egfp* fusion cassette was cloned downstream of the 1.6kb *i-fabp* promoter fragment. (C) The phosphorylation resistant *cagA*^{EPISA} allele lacks EPIYA motifs for phosphorylation by Src family kinases. (D) The *cagA*^{EPISA}*:egfp* fusion cassette was cloned downstream of the 5.3kb *b-actin* promoter fragment.

Fig. S2. CagA expression does not disrupt early intestinal morphology or cell polarity. Fluorescence micrograph of intestinal cross-sections of wild-type (A) and b-cagA (B) animals at 6 dpf showing green autofluorescence or staining with a pan-cadherin antibody.

Fig. S3. CagA expression does not result in increased inflammation Myeloperoxidase- (mpo) positive neutrophils present in the intestine at 8 dpf.

Fig. S4. Proposed mechanism for CagA-dependent overproliferation of the intestinal epithelium.

References

1. Blaser MJ, Atherton JC (2004) Helicobacter pylori persistence: biology and disease. J Clin Invest 113: 321-333.
2. Amieva MR, El-Omar EM (2008) Host-bacterial interactions in Helicobacter pylori infection. Gastroenterology 134: 306-323.
3. Peek RM, Jr., Blaser MJ (2002) Helicobacter pylori and gastrointestinal tract adenocarcinomas. Nat Rev Cancer 2: 28-37.
4. Asghar RJ, Parsonnet J (2001) Helicobacter pylori and risk for gastric adenocarcinoma. Semin Gastrointest Dis 12: 203-208.
5. Censini S, Lange C, Xiang Z, Crabtree JE, Ghiara P, et al. (1996) cag, a pathogenicity island of Helicobacter pylori, encodes type I-specific and disease-associated virulence factors. Proc Natl Acad Sci U S A 93: 14648-14653.
6. Bourzac KM, Guillemin K (2005) Helicobacter pylori-host cell interactions mediated by type IV secretion. Cell Microbiol 7: 911-919.
7. Selbach M, Moese S, Hauck CR, Meyer TF, Backert S (2002) Src is the kinase of the Helicobacter pylori CagA protein in vitro and in vivo. J Biol Chem 277: 6775-6778.
8. Stein M, Bagnoli F, Halenbeck R, Rappuoli R, Fantl WJ, et al. (2002) c-Src/Lyn kinases activate Helicobacter pylori CagA through tyrosine phosphorylation of the EPIYA motifs. Mol Microbiol 43: 971-980.
9. Amieva MR, Vogelmann R, Covacci A, Tompkins LS, Nelson WJ, et al. (2003) Disruption of the epithelial apical-junctional complex by Helicobacter pylori CagA. Science 300: 1430-1434.

10. Churin Y, Al-Ghoul L, Kepp O, Meyer TF, Birchmeier W, et al. (2003) Helicobacter pylori CagA protein targets the c-Met receptor and enhances the motogenic response. J Cell Biol 161: 249-255.

11. Higashi H, Tsutsumi R, Muto S, Sugiyama T, Azuma T, et al. (2002) SHP-2 tyrosine phosphatase as an intracellular target of Helicobacter pylori CagA protein. Science 295: 683-686.

12. Tsutsumi R, Higashi H, Higuchi M, Okada M, Hatakeyama M (2003) Attenuation of Helicobacter pylori CagA x SHP-2 signaling by interaction between CagA and C-terminal Src kinase. J Biol Chem 278: 3664-3670.

13. Mimuro H, Suzuki T, Tanaka J, Asahi M, Haas R, et al. (2002) Grb2 is a key mediator of helicobacter pylori CagA protein activities. Mol Cell 10: 745-755.

14. Suzuki M, Mimuro H, Kiga K, Fukumatsu M, Ishijima N, et al. (2009) Helicobacter pylori CagA phosphorylation-independent function in epithelial proliferation and inflammation. Cell Host Microbe 5: 23-34.

15. Franco AT, Israel DA, Washington MK, Krishna U, Fox JG, et al. (2005) Activation of beta-catenin by carcinogenic Helicobacter pylori. Proc Natl Acad Sci U S A 102: 10646-10651.

16. Barker N, Huch M, Kujala P, van de Wetering M, Snippert HJ, et al. (2010) Lgr5(+ve) stem cells drive self-renewal in the stomach and build long-lived gastric units in vitro. Cell Stem Cell 6: 25-36.

17. Sato T, van Es JH, Snippert HJ, Stange DE, Vries RG, et al. (2011) Paneth cells constitute the niche for Lgr5 stem cells in intestinal crypts. Nature 469: 415-418.

18. Pinto D, Gregorieff A, Begthel H, Clevers H (2003) Canonical Wnt signals are essential for homeostasis of the intestinal epithelium. Genes Dev 17: 1709-1713.

19. Ootani A, Li X, Sangiorgi E, Ho QT, Ueno H, et al. (2009) Sustained in vitro intestinal epithelial culture within a Wnt-dependent stem cell niche. Nat Med 15: 701-706.

20. Sato N, Meijer L, Skaltsounis L, Greengard P, Brivanlou AH (2004) Maintenance of pluripotency in human and mouse embryonic stem cells through activation of Wnt signaling by a pharmacological GSK-3-specific inhibitor. Nat Med 10: 55-63.

21. Oshima H, Matsunaga A, Fujimura T, Tsukamoto T, Taketo MM, et al. (2006) Carcinogenesis in mouse stomach by simultaneous activation of the Wnt signaling and prostaglandin E2 pathway. Gastroenterology 131: 1086-1095.

22. Powell SM, Zilz N, Beazer-Barclay Y, Bryan TM, Hamilton SR, et al. (1992) APC mutations occur early during colorectal tumorigenesis. Nature 359: 235-237.

23. Fearon ER, Vogelstein B (1990) A genetic model for colorectal tumorigenesis. Cell 61: 759-767.

24. El-Etr SH, Mueller A, Tompkins LS, Falkow S, Merrell DS (2004) Phosphorylation-independent effects of CagA during interaction between Helicobacter pylori and T84 polarized monolayers. J Infect Dis 190: 1516-1523.

25. Suzuki M, Mimuro H, Suzuki T, Park M, Yamamoto T, et al. (2005) Interaction of CagA with Crk plays an important role in Helicobacter pylori-induced loss of gastric epithelial cell adhesion. J Exp Med 202: 1235-1247.

26. Murata-Kamiya N, Kurashima Y, Teishikata Y, Yamahashi Y, Saito Y, et al. (2007) Helicobacter pylori CagA interacts with E-cadherin and deregulates the beta-catenin signal that promotes intestinal transdifferentiation in gastric epithelial cells. Oncogene 26: 4617-4626.

27. Wirth HP, Beins MH, Yang M, Tham KT, Blaser MJ (1998) Experimental infection of Mongolian gerbils with wild-type and mutant Helicobacter pylori strains. Infect Immun 66: 4856-4866.

28. Lee A, O'Rourke J, De Ungria MC, Robertson B, Daskalopoulos G, et al. (1997) A standardized mouse model of Helicobacter pylori infection: introducing the Sydney strain. Gastroenterology 112: 1386-1397.

29. Ohnishi N, Yuasa H, Tanaka S, Sawa H, Miura M, et al. (2008) Transgenic expression of Helicobacter pylori CagA induces gastrointestinal and hematopoietic neoplasms in mouse. Proc Natl Acad Sci U S A 105: 1003-1008.

30. Solnick JV, Canfield DR, Yang S, Parsonnet J (1999) Rhesus monkey (Macaca mulatta) model of Helicobacter pylori: noninvasive detection and derivation of specific-pathogen-free monkeys. Lab Anim Sci 49: 197-201.

31. Feng H, Stachura DL, White RM, Gutierrez A, Zhang L, et al. (2010) T-lymphoblastic lymphoma cells express high levels of BCL2, S1P1, and ICAM1, leading to a blockade of tumor cell intravasation. Cancer Cell 18: 353-366.

32. Ceol CJ, Houvras Y, Jane-Valbuena J, Bilodeau S, Orlando DA, et al. (2011) The histone methyltransferase SETDB1 is recurrently amplified in melanoma and accelerates its onset. Nature 471: 513-517.

33. White RM, Cech J, Ratanasirintrawoot S, Lin CY, Rahl PB, et al. (2011) DHODH modulates transcriptional elongation in the neural crest and melanoma. Nature 471: 518-522.

34. Haramis AP, Hurlstone A, van der Velden Y, Begthel H, van den Born M, et al. (2006) Adenomatous polyposis coli-deficient zebrafish are susceptible to digestive tract neoplasia. EMBO Rep 7: 444-449.

35. Muncan V, Faro A, Haramis AP, Hurlstone AF, Wienholds E, et al. (2007) T-cell factor 4 (Tcf7l2) maintains proliferative compartments in zebrafish intestine. EMBO Rep 8: 966-973.

36. Tsukamoto T, Mizoshita T, Mihara M, Tanaka H, Takenaka Y, et al. (2005) Sox2 expression in human stomach adenocarcinomas with gastric and gastric-and-intestinal-mixed phenotypes. Histopathology 46: 649-658.

37. Tissier-Seta JP, Mucchielli ML, Mark M, Mattei MG, Goridis C, et al. (1995) Barx1, a new mouse homeodomain transcription factor expressed in cranio-facial ectomesenchyme and the stomach. Mech Dev 51: 3-15.

38. Kim BM, Buchner G, Miletich I, Sharpe PT, Shivdasani RA (2005) The stomach mesenchymal transcription factor Barx1 specifies gastric epithelial identity through inhibition of transient Wnt signaling. Dev Cell 8: 611-622.

39. Crosnier C, Vargesson N, Gschmeissner S, Ariza-McNaughton L, Morrison A, et al. (2005) Delta-Notch signalling controls commitment to a secretory fate in the zebrafish intestine. Development 132: 1093-1104.

40. Cheesman SE, Neal JT, Mittge E, Seredick BM, Guillemin K (2010) Epithelial cell proliferation in the developing zebrafish intestine is regulated by the Wnt pathway and microbial signaling via Myd88. Proc Natl Acad Sci U S A 108 Suppl 1: 4570-4577.

41. Faro A, Boj SF, Clevers H (2009) Fishing for intestinal cancer models: unraveling gastrointestinal homeostasis and tumorigenesis in zebrafish. Zebrafish 6: 361-376.

42. Guillemin K, Salama NR, Tompkins LS, Falkow S (2002) Cag pathogenicity island-specific responses of gastric epithelial cells to Helicobacter pylori infection. Proc Natl Acad Sci U S A 99: 15136-15141.

43. Segal ED, Cha J, Lo J, Falkow S, Tompkins LS (1999) Altered states: involvement of phosphorylated CagA in the induction of host cellular growth changes by Helicobacter pylori. Proc Natl Acad Sci U S A 96: 14559-14564.

44. Higashijima S, Okamoto H, Ueno N, Hotta Y, Eguchi G (1997) High-frequency generation of transgenic zebrafish which reliably express GFP in whole muscles or the whole body by using promoters of zebrafish origin. Dev Biol 192: 289-299.

45. Her GM, Chiang CC, Wu JL (2004) Zebrafish intestinal fatty acid binding protein (I-FABP) gene promoter drives gut-specific expression in stable transgenic fish. Genesis 38: 26-31.

46. Ng AN, de Jong-Curtain TA, Mawdsley DJ, White SJ, Shin J, et al. (2005) Formation of the digestive system in zebrafish: III. Intestinal epithelium morphogenesis. Developmental biology 286: 114-135.

47. Nagy TA, Wroblewski LE, Wang D, Piazuelo MB, Delgado A, et al. (2011) beta-Catenin and p120 Mediate PPARdelta-Dependent Proliferation Induced by Helicobacter pylori in Human and Rodent Epithelia. Gastroenterology 141: 553-564.

48. He TC, Sparks AB, Rago C, Hermeking H, Zawel L, et al. (1998) Identification of c-MYC as a target of the APC pathway. Science 281: 1509-1512.

49. Yan D, Wiesmann M, Rohan M, Chan V, Jefferson AB, et al. (2001) Elevated expression of axin2 and hnkd mRNA provides evidence that Wnt/beta -catenin signaling is activated in human colon tumors. Proc Natl Acad Sci U S A 98: 14973-14978.

50. Tetsu O, McCormick F (1999) Beta-catenin regulates expression of cyclin D1 in colon carcinoma cells. Nature 398: 422-426.

51. Heisenberg CP, Houart C, Take-Uchi M, Rauch GJ, Young N, et al. (2001) A mutation in the Gsk3-binding domain of zebrafish Masterblind/Axin1 leads to a fate transformation of telencephalon and eyes to diencephalon. Genes Dev 15: 1427-1434.

52. van de Water S, van de Wetering M, Joore J, Esseling J, Bink R, et al. (2001) Ectopic Wnt signal determines the eyeless phenotype of zebrafish masterblind mutant. Development 128: 3877-3888.

53. Nobili S, Bruno L, Landini I, Napoli C, Bechi P, et al. (2011) Genomic and genetic alterations influence the progression of gastric cancer. World journal of gastroenterology : WJG 17: 290-299.

54. Ranzani GN, Luinetti O, Padovan LS, Calistri D, Renault B, et al. (1995) p53 gene mutations and protein nuclear accumulation are early events in intestinal type gastric cancer but late events in diffuse type. Cancer epidemiology, biomarkers & prevention : a publication of the American Association for Cancer Research, cosponsored by the American Society of Preventive Oncology 4: 223-231.

55. Shibata A, Parsonnet J, Longacre TA, Garcia MI, Puligandla B, et al. (2002) CagA status of Helicobacter pylori infection and p53 gene mutations in gastric adenocarcinoma. Carcinogenesis 23: 419-424.

56. Buti L, Spooner E, Van der Veen AG, Rappuoli R, Covacci A, et al. (2011) Helicobacter pylori cytotoxin-associated gene A (CagA) subverts the apoptosis-stimulating protein of p53 (ASPP2) tumor suppressor pathway of the host. Proc Natl Acad Sci U S A 108: 9238-9243.

57. Storer NY, Zon LI (2010) Zebrafish models of p53 functions. Cold Spring Harbor perspectives in biology 2: a001123.

58. Berghmans S, Murphey RD, Wienholds E, Neuberg D, Kutok JL, et al. (2005) tp53 mutant zebrafish develop malignant peripheral nerve sheath tumors. Proc Natl Acad Sci U S A 102: 407-412.

59. Higashi H, Nakaya A, Tsutsumi R, Yokoyama K, Fujii Y, et al. (2004) Helicobacter pylori CagA induces Ras-independent morphogenetic response through SHP-2 recruitment and activation. J Biol Chem 279: 17205-17216.

60. El-Omar EM, Rabkin CS, Gammon MD, Vaughan TL, Risch HA, et al. (2003) Increased risk of noncardia gastric cancer associated with proinflammatory cytokine gene polymorphisms. Gastroenterology 124: 1193-1201.

61. Kwan KM, Fujimoto E, Grabher C, Mangum BD, Hardy ME, et al. (2007) The Tol2kit: a multisite gateway-based construction kit for Tol2 transposon transgenesis constructs. Dev Dyn 236: 3088-3099.

62. Westerfield M (2007) The Zebrafish Book. University of Oregon Press 4th Edition.

63. Ruijter JM, Ramakers C, Hoogaars WM, Karlen Y, Bakker O, et al. (2009) Amplification efficiency: linking baseline and bias in the analysis of quantitative PCR data. Nucleic Acids Res 37: e45.

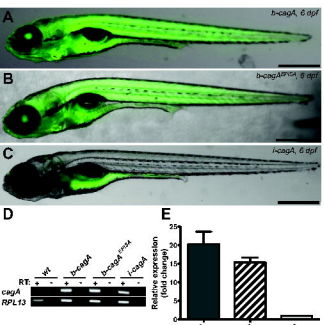
A
b-cagA, 6 dpf
B
b-cagAΔrmsA, 6 dpf
C
i-cagA, 6 dpf
D
WT
b-cagA
b-cagAΔrmsA
i-cagA
RT:
cagA
RPL13
E
Relative transcription (fold change)
25
20
15
10
5
0
b-cagA
b-cagAΔrmsA
i-cagA

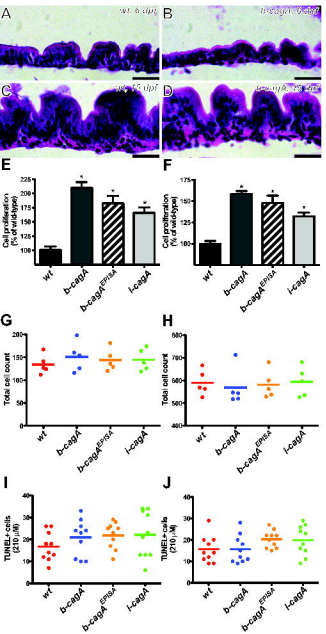
A
B
C
D
E
F
Cell proliferation (% of wt/dpa)
wt
b-cagA
b-cagA^EPISA
i-cagA
G
H
Total cell count
I
J
TUNEL+ cells (210 µM)

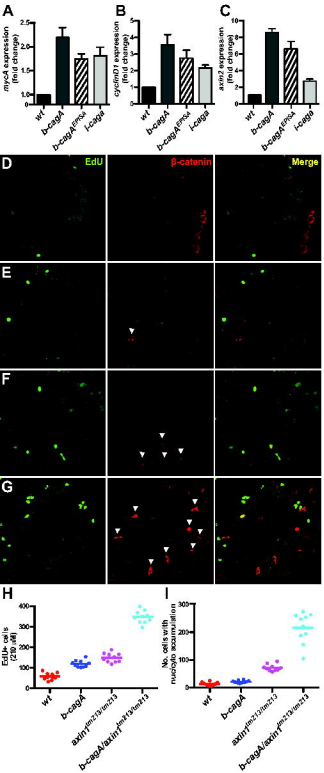
A
mycA expression (fold change)
wt
b-cagA
b-cagA^mosa
i-cagA
B
cyclinD1 expression (fold change)
wt
b-cagA
b-cagA^mosa
i-cagA
C
axin2 expression (fold change)
wt
b-cagA
b-cagA^mosa
i-cagA
D
EdU
β-catenin
Merge
E
F
G
H
EdU+ cells (cells/ul)
wt
b-cagA
axin1^mz219/mz219
b-cagA/axin1^mz219/mz219
I
No. cells with nuclear accumulation
wt
b-cagA
axin1^mz219/mz219
b-cagA/axin1^mz219/mz219

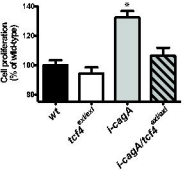
Cell proliferation
(% of wild-type)
140
120
100
80
*
wt
tcf4 ΔCtercl
i-cagA
i-cagA/tcf4 ΔCterl

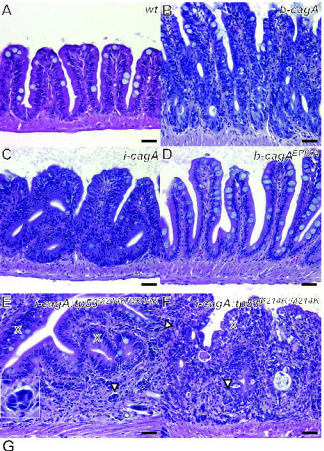
A
wt
B
b-cagA
C
i-cagA
D
b-cagA^ΔEPIYA
E
b-cagA
F
b-cagA

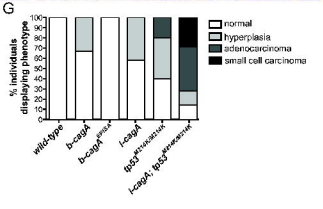
G
% individuals displaying phenotype
100
90
80
70
60
50
45
30
20
10
0
normal
hyperplasia
adenocarcinoma
small cell carcinoma
wild-type
b-cagA
b-cagA^ΔEPIYA
i-cagA
tp53^KN/KN;Lox
i-cagA; tp53^KN/KN;Lox